

Data Acquisition

2.1 RATIONALE

Unless we use simulated signals, data acquisition necessarily precedes signal processing. In any recording setup, the devices that are interconnected and coupled to the biological process form a so-called measurement chain. In Chapter 1, we discussed the acquisition of a waveform via an amplifier and analog-to-digital converter (ADC) step (see Fig. 1.6). Here we elaborate on the process of data acquisition by looking at the role of the components in the measurement chain in more detail (Fig. 2.1).

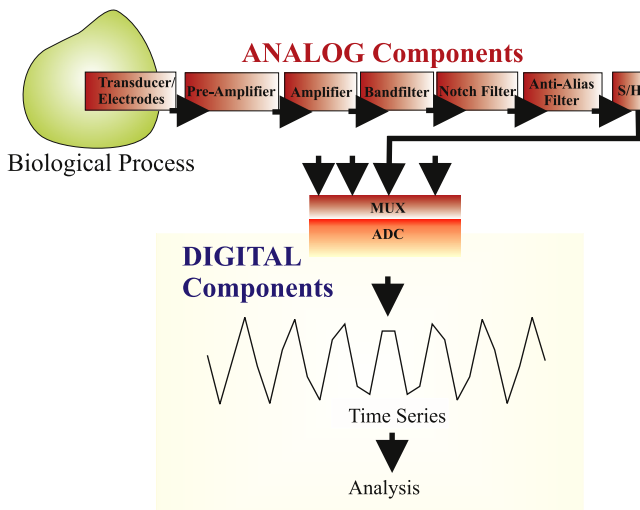


FIGURE 2.1 Diagram of a data acquisition setup, the measurement chain. The modules up to the analog-to-digital converter (ADC) are analog devices, while the remaining components are the digital devices. *MUX*, multiplexer; *S/H*, sample hold module.

In-depth knowledge of the measurement process is often critical for effective data analysis, because each type of data acquisition system is associated with specific artifacts and problems. Technically accurate measurement and proper treatment of artifacts are essential for data processing; these steps guide the selection of the processing strategies, the interpretation of results, and allow one to avoid the “*garbage in = garbage out*” trap that comes with every type of data analysis.

2.2 THE MEASUREMENT CHAIN

Most acquisition systems can be subdivided into analog and digital components (Fig. 2.1). The analog part of the measurement chain conditions the signal (through amplification, filtering, etc.) prior to the A/D conversion. Observing a biological process normally starts with the connection of a transducer or electrode pair to pick up a signal. Usually, the next stage in a measurement chain is amplification. In most cases the amplification takes place in two steps using a separate preamplifier and amplifier. After amplification, the signal is usually filtered to attenuate undesired frequency components. This can be done by passing the signal through a bandpass filter and/or by cutting out specific frequency components (using a band reject, or notch filter) such as a 60-Hz hum. A critical step is to attenuate frequencies that are too high to be digitized by the ADC. This operation is performed by the antialiasing filter. Finally, the sample-and-hold (S/H) circuit samples the analog signal and holds it to a constant value during the ADC process. The diagram in Fig. 2.1 represents a basic acquisition setup in which some functions can be interchanged, omitted, or moved into the digital domain; this will be discussed in Section 2.4.

The goal of the acquisition setup is to measure biological signals as “cleanly” (with as little noise) as possible, without significant interactions due to the measurement itself. For instance, if a bioelectrical response is to be measured, we want to *establish the correct amplitude* of the bio-potential without *influencing (i.e., stimulating or inhibiting) the system with current originating from the equipment*.

2.2.1 Analog Components

In the analog part of the measurement chain, one normally connects different instruments to obtain an analog signal with appropriate characteristics for the ADC (Fig. 2.1). As will be outlined in the following, when connecting equipment, one has to follow the rule of *low output impedance—high input impedance*. As Fig. 2.2 shows, any element in the

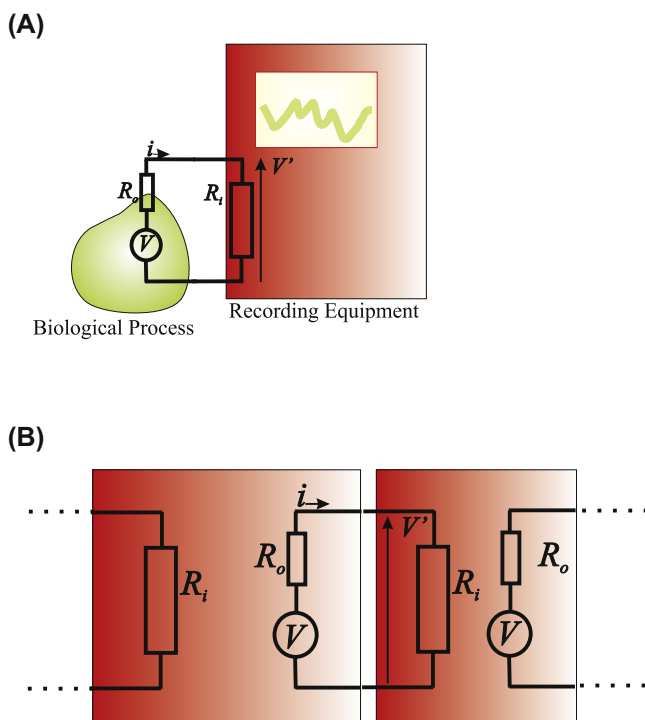


FIGURE 2.2 Equivalent circuit representation of elements in a measurement chain. (A) A simplified situation in which a biological process is directly coupled to an oscilloscope. (B) A generic diagram of coupling devices in a chain.

chain can be represented as a black box with an input and output resistance. The situation in Fig. 2.2A is a biological preparation generating a biopotential coupled via direct electrical contact to an oscilloscope screen displaying the measured signal. In this example, the biopotential (V) is associated with a current (i) that is (according to Ohm's law) determined by R_o (the output resistance) and R_i (the input resistance).

$$i = \frac{V}{R_i + R_o} \quad (2.1)$$

Ideally one would like to measure V without drawing any current (i) from the biological process itself. Because it is impossible to measure a potential without current, at best we can minimize the current drawn from our preparation at any given value of the biopotential (V); *therefore considering Eq. (2.1) we may conclude that $R_i + R_o$ must be large to minimize current flow within the preparation from our instruments.*

The other concern is to obtain a reliable measurement reflecting the true biopotential. The oscilloscope in Fig. 2.2A cannot measure the exact value because the potential is attenuated over both the output and input resistors. The potential V' in the oscilloscope relates to the real potential V as:

$$V' = \frac{R_i}{R_i + R_o} V \quad (2.2)$$

V' is close to V if $R_i \gg R_o$ producing an attenuation factor that approaches 1.

The basic concepts in this example apply not only for the first step in the measurement chain, but also for any connection in a chain of instruments (Fig. 2.2B). Specifically, a high input resistance combined with a low output resistance ensures that:

1. no significant amount of current is drawn;
2. the measured value at the input represents the output of the previous stage.

Measurements of biopotentials are not trivial since the electrodes themselves constitute a significant resistance and capacitance (Fig. 2.3), usually indicated as electrode impedance. Electroencephalogram (EEG) electrodes on the skin have an impedance of about $5\text{ k}\Omega$ (typically measured at 20–30 Hz); microelectrodes that are used in most basic electrophysiology studies have an impedance from several hundreds of $\text{k}\Omega$ up to several $\text{M}\Omega$ (measured at around 1 kHz). This isn't an ideal starting point; constraint (1) above will be easily satisfied (the electrodes by themselves usually have a high impedance which limits the current) but constraint (2) is a bit more difficult to meet. This problem can only be resolved by including a primary amplifier stage with an input-impedance that is extremely high, i.e., several orders of magnitude above the electrode's impedance. This is the main function of the preamplifier or head

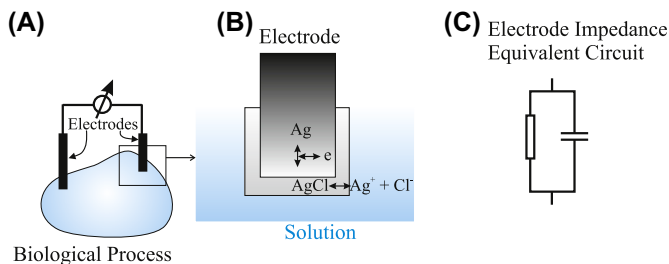


FIGURE 2.3 Components of typical biopotential measurement. (A) A setup with silver–silver chloride electrodes with (B) a detail of the chloride layer and (C) a simplified electronic equivalent circuit.

stage in measurement setups. For this reason these devices are sometimes referred to as impedance transformers: the input impedance is extremely high while the output impedance of the head stage is only several Ω .

In electrophysiology experiments, metal electrodes are often used to measure potentials from biological specimens which must be bathed in an ionic solution. A fundamental problem with such direct measurements of electricity in solutions is the interface between the metal and solution. This boundary generates an electrode potential that is material and solution specific. The electrode potential is usually not a problem when biopotentials are read from electrode pairs made of the same material. In cases where the metal and solutions are not the same for both electrodes, the DC offset generated at the electrode–solution interface can usually be corrected electronically in the recording equipment. Somewhat more problematically, the metal–fluid boundary can act as an impedance with a significant capacitive element (Fig. 2.3C). This capacitance may degrade the signal by blocking the low-frequency components. One widely used approach to mitigate this problem is to use a silver electrode with a silver chloride coating. This facilitates the transition from ionic (Ag^+ or Cl^- ; Fig. 2.3B) to electronic (e; Fig. 2.3B) conduction, reducing the electrode capacitance at the solution interface, and consequently facilitating the recording of signals with low-frequency components.

The purpose of amplification in the analog domain is to increase the signal level to match the range of the ADC. Unfortunately, since amplifiers increase the level of both desirable and undesirable elements of signals, additional procedures are often required to reduce noise contamination. This is typically accomplished with analog filtering before, or digital filtering after, the ADC. With the exception of the anti-aliasing filter, the replacement of analog filters with digital filters is equivalent from a signal processing point of view. The purpose of the *antialiasing filter* in the analog part of the measurement chain is to prevent the system from creating erroneous signals at the ADC. This will be explained in the Sections 2.2.2 and 2.3.

So far we have considered the acquisition of a single channel of data. In real recording situations one is frequently interested in multiple channels. Recordings of clinical EEG typically vary between 20 and 32 channels, and electrocorticogram (ECoG) measurements often include more than 100 channels. These channels are usually digitized by a limited number of ADCs, with each ADC connected to a set of input channels via a multiplexer (MUX; Fig. 2.1), a high-speed switch that sequentially connects these channels to the ADC. Because each channel is digitized in turn, a small time lag between the channels may be introduced at conversion. In most cases with modern equipment, where the switching and conversion times are small, no compensation for these time shifts is necessary. However, with a relatively slow, multiplexed A/D converter, a so-called

sample-and-hold unit must be included in the measurement chain (Fig. 2.1). An array of these units can hold sampled values from several channels during the conversion process, thus preventing the converter from “chasing” a moving target and avoiding a time lag between data streams in a multichannel measurement.

2.2.2 Analog to Digital Conversion

ADC can be viewed as imposing a grid on a continuous signal (see Fig. 1.6). The signal becomes discrete both in *amplitude* and *time*. It is obvious that the grid must be sufficiently fine and must cover the full extent of the signal to avoid a significant loss of information.

The discretization of the signal in the *amplitude* dimension is determined by the converter’s input voltage range and the analog amplification of the signal input to it (Chapter 1, Fig. 1.6). As an example: we have a 12-bit converter with an input-range of 5V and an analog measurement chain with a preamplifier that amplifies $100\times$ and a second-stage amplifier that amplifies $100\times$. The result is a total amplification of 10,000, translating into $(5\text{V} \div 10,000 =) 500\text{ }\mu\text{V}$ *range* for the input of the acquisition system. The converter has 2^{12} steps (4096), resulting in a *resolution* at the input of $(500\text{ }\mu\text{V} \div 4096 = 0.12\text{ }\mu\text{V})$. It may seem that an ADC with a greater bit depth is better because it generates samples at a higher precision. However, sampling at this higher precision in the ADC may be inefficient because it requires a lot of memory to store the acquired data, without providing any additional information about the underlying biological process. In such a case all the effort is wasted on storing noise. Therefore, in real applications, there is a trade-off between resolution, range, and storage capacity.

At conversion, the amplitude of the analog signal is approximated by the discrete levels of the ADC. Depending on the type of converter this approximation may behave numerically as a truncation or as a round-off of the continuous-valued signal to an integer. In both cases one can consider the quantization as a source of noise in the measurement system, noise which is directly related to the resolution at the ADC (*quantization noise*, Chapter 3).

The continuous signal is also discretized (sampled) in *time*. To obtain a reliable sampled representation of a continuous signal, the sample interval (T_s) or sample frequency ($F_s = 1/T_s$) must relate to the type of signal that is being recorded. In order to develop a mathematical description of sampling, we introduce the unit impulse (Dirac impulse) function δ .

The plots in Fig. 2.4A show how the unit step and unit impulse functions can be thought of as a ramp function and its derivative, respectively, in the limit as the ramp width τ approaches 0. In terms of the amplitude

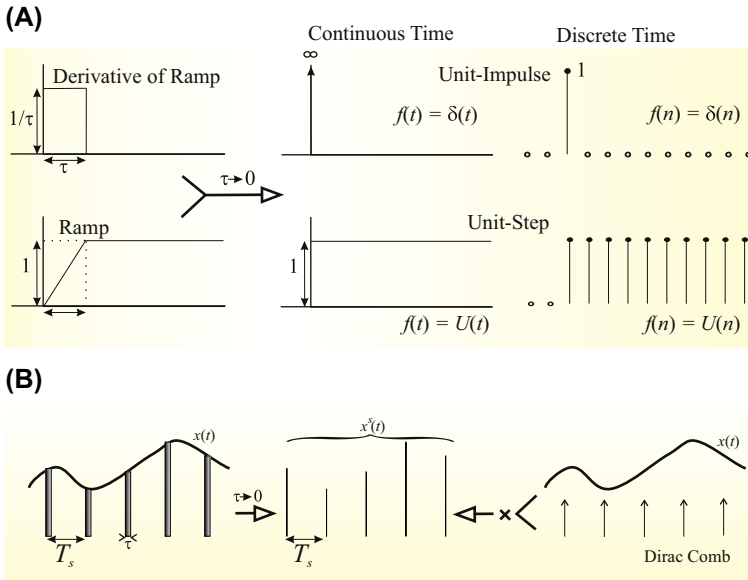


FIGURE 2.4 Graphical representation of the Dirac δ in continuous and discrete time. (A) The unit impulse (δ , top row) and unit step (U , bottom row) function. The unit impulse can be considered as the derivative of the unit step. The unit impulse can be considered a square wave with duration τ and amplitude $1/\tau$ in which $\tau \rightarrow 0$. Note also that in continuous time the amplitude of the unit impulse is ∞ , whereas the amplitude is 1 in the discrete time version. Here both the impulse and step functions are derived from the ramp function, though other approaches exist (e.g., Chapter 20). (B) Sampling a continuous function $x(t)$ by multiplication with the Dirac comb generates discrete time function $x^s(t)$.

$\delta(0)$, the unit impulse (Dirac) function at 0, behaves a bit differently for the continuous (∞) and discrete time (1) versions. The unit step functions in discrete and continuous time both have amplitudes of 1.

The Dirac delta function in the integral and summation expressions in Table 2.1 can be used to sample a continuous function $x(t)$ at $t = 0$. If we

TABLE 2.1 Dirac Delta Function

Continuous Time	Discrete Time
$\delta(t) = 0$ for $t \neq 0$	$\delta(n) = 0$ for $n \neq 0$
$\int_{-\infty}^{\infty} \delta(t) dt = 1$	$\sum_{n=-\infty}^{\infty} \delta(n) = 1$

define the top-left function in Fig. 2.4A (a square wave with duration τ and amplitude $1/\tau$) as the approximation δ_τ for δ , we can state:

$$\int_{-\infty}^{\infty} x(t)\delta(t)dt = \lim_{\tau \rightarrow 0} \int_{-\infty}^{\infty} x(t)\delta_\tau(t)dt \quad (2.3)$$

Because $\delta_\tau(t) = 0$ outside the $0 \rightarrow \tau$ interval, we can change the upper and lower limits of the integration:

$$\lim_{\tau \rightarrow 0} \int_{-\infty}^{\infty} x(t)\delta_\tau(t)dt = \lim_{\tau \rightarrow 0} \int_0^{\tau} x(t)\delta_\tau(t)dt \quad (2.4)$$

Within these limits, $\delta_\tau(t) = \frac{1}{\tau}$; therefore we obtain:

$$\lim_{\tau \rightarrow 0} \int_0^{\tau} x(t)\delta_\tau(t)dt = \lim_{\tau \rightarrow 0} \int_0^{\tau} \frac{x(t)}{\tau} dt \quad (2.5)$$

If we now use $\tau \rightarrow 0$, so that $x(t)$ becomes $x(0)$, which can be considered a constant and not a function of t anymore, we can evaluate the integral:

$$\lim_{\tau \rightarrow 0} \int_0^{\tau} \frac{x(t)}{\tau} dt = \lim_{\tau \rightarrow 0} x(0) \underbrace{\int_0^{\tau} \frac{1}{\tau} dt}_1 = x(0) \quad (2.6)$$

Because the integral evaluates to 1 and combining the result with our starting point in Eq. (2.3), we conclude:

$$x(0) = \int_{-\infty}^{\infty} x(t)\delta(t)dt \quad (2.7)$$

Here we assumed that the integral for the δ function remains 1 even as $\tau \rightarrow 0$. The reasoning we followed to obtain the result above isn't the most rigorous, but it makes it a plausible case for the integral in Eq. (2.7) evaluating to $x(0)$.

By using $\delta(t - \Delta)$ instead of $\delta(t)$, we obtain the value of a function at $t = \Delta$ instead of $x(0)$. If we now consider a function evaluated at arbitrary values of delay Δ , we obtain the so-called *sifting property* of the unit impulse function:

$$x(\Delta) = \int_{-\infty}^{\infty} x(t)\delta(t - \Delta)dt \quad (2.8)$$

Using this property, we can sift out specific values of a continuous function $x(t)$ at given values of t . As we will see in the remainder of this text, this property of the delta function is frequently used to evaluate integrals including the δ function.

The Dirac δ function is used to formalize the sampling of a continuous time function. We can depict this sampling procedure as a continuous time function $x(t)$ that is sampled over very short time intervals τ at regular intervals T_s , and that is considered zero in between the sampling times (Fig. 2.4B). Each of the gray rectangles at time instant nT_s in the left plot in Fig. 2.4B can be considered as an approximation of the Dirac delta $\delta_\tau(t - nT_s)$ that is weighted by the value of $x(t)$ at $t = nT_s$, i.e., each sample value at $t = nT_s$ equals $x(nT_s)\delta_\tau(t - nT_s)$. If we add all individual samples (sampling the whole function $x(t)$ at regular intervals separated by T_s), we get the **sampled representation** x^s , which can be written as: $\sum_{n=-\infty}^{\infty} x(nT_s)\delta_\tau(t - nT_s)$. If we subsequently let $\tau \rightarrow 0$, then the approximated delta function δ_τ approaches the true δ . Each impulse at $t = nT_s$ is weighted by $x(nT_s)$. The representation of the sampled function now looks like the middle panel in Fig. 2.4B, where the sampled function x^s is represented by very brief pulses of amplitude $x(nT_s)$ and zero in between these pulses. Following this reasoning we make it plausible to represent the sampled equivalent of continuous time function x as x^s :

$$x^s(nT_s) = \sum_{n=-\infty}^{\infty} x(nT_s)\delta(t - nT_s) = x(t) \sum_{n=-\infty}^{\infty} \delta(t - nT_s) \quad (2.9)$$

In the above equation we took the liberty of replacing $x(nT_s)$ with $x(t)$, i.e., we used the equality $x(nT_s)\delta(t - nT_s) = x(t)\delta(t - nT_s)$. This again is a plausible step because the delta function $\delta(t - nT_s)$ equals zero for all $t \neq nT_s$, so including values of $x(t)$ other than $t = nT_s$ does not affect the outcome of the product. The expression $\sum_{n=-\infty}^{\infty} \delta(t - nT_s)$ represents a series of Diracs at regular intervals and is often called the **Dirac comb** δ_{T_s} (Fig. 2.4B right panel). Because the sample interval T_s is usually a constant, it is often omitted, thereby indicating x^s as a function of n only. Finally, we obtain the commonly used representation of a sampled function as the product of a Dirac comb and the continuous time function (Fig. 2.4B):

$$\boxed{x^s(n) = x(t)\delta_{T_s}} \quad (2.10)$$

Again, the procedures we used above to introduce the properties of the Dirac functions in Eqs. (2.8) and (2.9) were more intuitive than mathematically rigorous; though the reasoning underlying these properties can be made rigorous using distribution theory, which is not further discussed in this text.

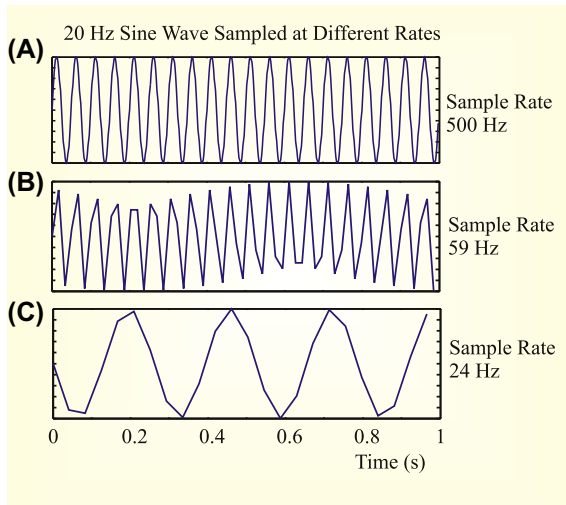


FIGURE 2.5 Sampling a 20-Hz sine wave at different rates $F_s = 1/T_s$. The effects shown in this figure can be further examined with the MATLAB® `pr2_1.m` script. F_s , sample rate; T_s , sample interval.

From time domain observation, it may be obvious that the sample rate at which one obtains $x^s(t)$ must be sufficient to represent the change in the continuous signal $x(t)$. Several examples are shown in Fig. 2.5. As illustrated schematically in the figure, it seems that sampling a 20-Hz sine wave at a rate of $2 \times 20 = 40$ Hz at least conserves the frequency content of the signal. If these samples were taken exactly at the peaks and valleys of the sine wave, the sampled wave would look like a 20-Hz triangular wave. If not sampled at the peaks and valleys, the waveform will have an even more severely distorted appearance.

The waves in Fig. 2.5 are examples created with `pr2_1.m` in MATLAB®.

```
% pr2_1.m
% Aliasing
% example signal
t=0:0.001:1;           % 1 sec divided into ms steps
f=20;                  % Frequency in Hertz
signal=sin(2*pi*f*t);

% Simulate different sample rates and plot
figure
for skip=2:5:50;
    plot(t,signal,'r'); hold;      % The Original Signal
    plot(t(1:skip:1000),signal(1:skip:1000));
```

```
tt=['Sine' num2str(f) ' Hz: space bar to continue: SAMPLE RATE = '  
    num2str(1000/skip)];  
title(tt);  
drawnow  
pause;  
clf;  
end;
```

If you need to refresh or practice your MATLAB® skills, do one of the introductory courses or see a text such as [Ingle and Proakis \(1997\)](#) or [Wallisch et al. \(2014\)](#). Running the preceding program shows the original waveform in red and the simulated sampled version in blue. Press “Enter” to see subsequent lower sample rates. The minimum sampling rate (in this example 40 Hz) is called the *Nyquist sampling frequency* or the *Nyquist limit*. Thus, the sampling rate determines the highest frequency that can be represented by the sampled signal. This value (half the sample rate) is often indicated as the *Nyquist frequency* of the sampled signal.

In the example in [Fig. 2.5](#) the highest frequency in the signal is 20 Hz, requiring a sample rate >40 Hz. The Nyquist limit is a real bare minimum to capture the 20-Hz frequency component and you can see in the figure that the wave morphology is already distorted at sample rates close to, but above, the Nyquist sampling frequency (e.g., 59 Hz in [Fig. 2.5B](#)). Clearly the signal is seriously misrepresented below the Nyquist limit (e.g., 24 Hz in [Fig. 2.5C](#)). This particular type of signal distortion is called *aliasing*: the example in [Fig. 2.5](#) shows a signal of ~ 4 Hz that is an alias of the real 20-Hz signal resulting from undersampling.

To remove the effect of aliasing in digitized signals, the analog measurement chain must remove/attenuate all frequencies above the Nyquist frequency by using a filter (*antialiasing filter*). To avoid distortion in the time domain (as seen in the example where the wave is digitized at 59 Hz) sampling at ~ 5 times the maximum frequency is not uncommon.

Note: Aliasing is not a phenomenon that occurs only at the ADC, but at all instances where a signal is made discrete. It may also be observed when waves are represented on a screen or on a printout with a limited number of pixels. It is also not restricted to time series but also occurs when depicting images (2-D signals) in a discrete fashion.

2.3 SAMPLING AND NYQUIST FREQUENCY IN THE FREQUENCY DOMAIN

This section considers the Nyquist sampling theorem in the frequency domain. Unfortunately, this explanation in its simplest form requires a background in the Fourier transform and convolution, both topics that will be discussed later (see Chapters 5–7, 13). For readers who are not yet familiar with these topics, it is advised to skip this section and return to it later. In this section we approach sampling in the frequency domain somewhat intuitively, and focus on the general principles depicted in Fig. 2.6. A more formal treatment of the sampling problem can be found in Appendix 2.1.

When sampling a function $f(t)$, using the property of the δ function (Eq. 2.9), we multiply the continuous time function with a Dirac comb, a series of unit impulses with regular interval T_s :

$$\text{Sampled function : } f(t) \sum_{n=-\infty}^{\infty} \delta(t - nT_s) \quad (2.11)$$

As will be discussed in Chapter 13, multiplication in the time domain is equivalent to a convolution (\otimes) in the frequency domain, i.e.:

$$F(f) \otimes \Delta(f) \quad \text{with : } F(f) \Leftrightarrow f(t) \quad \text{and} \quad \Delta(f) \Leftrightarrow \sum_{n=-\infty}^{\infty} \delta(t - nT_s) \quad (2.12)$$

The double arrow \Leftrightarrow in Eq. (2.12) separates a Fourier transform pair: here the frequency domain is left of the arrow and the time domain equivalent is the expression on the right of \Leftrightarrow . We can use the sifting property to evaluate the Fourier transform integral of a single delta function:

$$\delta(t) \Leftrightarrow \int_{-\infty}^{\infty} \delta(t) e^{-2\pi f t} dt = e^0 = 1 \quad (2.13)$$

For the series of impulses (the Dirac comb) the transform $\Delta(f)$ is a more complex expression, according to the definition of the Fourier transform (Eq. 6.4, Chapter 6):

$$\Delta(f) = \int_{-\infty}^{\infty} \sum_{n=-\infty}^{\infty} \delta(t - nT_s) e^{-2\pi f t} dt \quad (2.14)$$

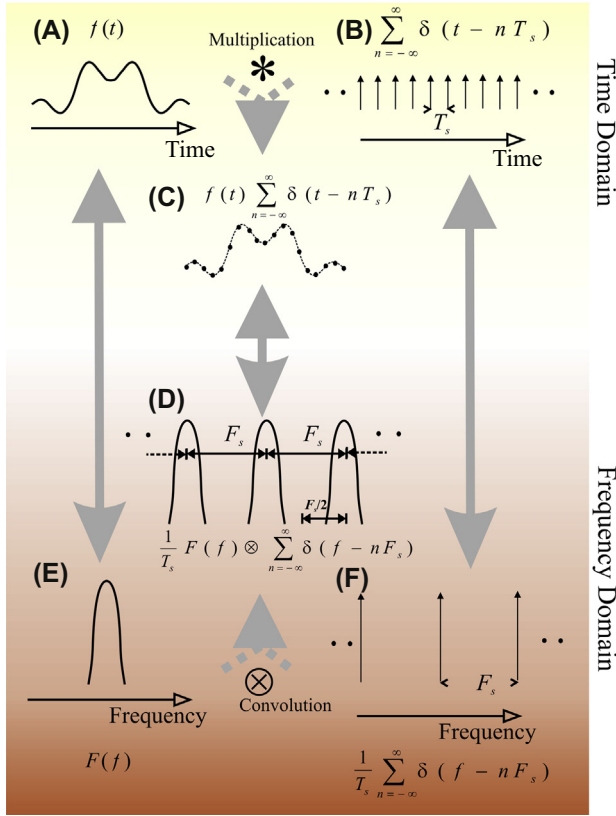


FIGURE 2.6 Fourier transform of a sampled function. Sampling a function $f(t)$ (A) in the time domain can be represented by a multiplication (*) of $f(t)$ with a train of δ functions with an interval T_s , as depicted in (B), resulting in a series of samples (C). The Fourier transform of the sampled version is a periodic function, as shown in (D). The Fourier transform of the sampled function can be obtained from the convolution (\otimes) of the Fourier transform $F(f)$ of $f(t)$ (shown in (E)) and the Fourier transform of the train of unit impulses with an interval $F_s = 1/T_s$, as shown in (F). From this diagram it can be appreciated that the width of $F(f)$ should fall within period F_s (i.e., the maximum value of the spectrum of the sampled signal must be less than $F_s/2$) in order to avoid overlap in the spectra (shown in Fig. 2.7). Further details can be found in [Appendix 2.1](#).

Assuming that we can interchange the summation and integral operations, and using the sifting property again, the above expression evaluates to:

$$\sum_{n=-\infty}^{\infty} \int_{-\infty}^{\infty} \delta(t - nT_s) e^{-2\pi f t} dt = \sum_{n=-\infty}^{\infty} e^{-2\pi f n T_s} \quad (2.15)$$

An essential difference between this expression and the Fourier transform of a single δ function, is the summation for n from $-\infty$ to ∞ . Changing the sign of the exponent in Eq. (2.15) is equivalent to changing the order of the summation from $-\infty \rightarrow \infty$ to $\infty \rightarrow -\infty$. Therefore we may state:

$$\sum_{n=-\infty}^{\infty} e^{-2\pi f n T_s} = \sum_{n=-\infty}^{\infty} e^{2\pi f n T_s} \quad (2.16)$$

From Eq. (2.16) it can be established that the sign of the exponent in Eqs. (2.13) to (2.16) doesn't matter. Thinking about this a bit: taking into account the similarity between the Fourier transform and the inverse transform integrals (Eqs. 6.4 and 6.8 in Chapter 6), the main difference of the integral being the sign of the exponent, this indicates that the Fourier transform and the inverse Fourier transform of a Dirac comb must evaluate to a similar form. This leads to the conclusion that the (inverse) Fourier transform of a Dirac comb must be another Dirac comb. Given that in the *time domain* we have: $\sum_{n=-\infty}^{\infty} \delta(t - nT_s)$, its Fourier transform in the *frequency domain* must be proportional to $\sum_{n=-\infty}^{\infty} \delta(f - nF_s)$. In these expressions the sample frequency $F_s = 1/T_s$. If you feel that this "proof" is too informal, please consult [Appendix 2.1](#) for a more thorough approach. You will find there that I am indeed ignoring a scaling factor equal to $1/T_s$ in the above expression (see [Eq. \(A2.1-7\)](#) in [Appendix 2.1](#)).

We will not worry about this scaling factor here; because for sample rate issues, we are interested in timing and not amplitude. For now we can establish the relationship between the Fourier transform $F(f)$ of a function $f(t)$ and the Fourier transform of its sampled version. Using the obtained result and [Eq. \(2.12\)](#), we find that the sampled version is proportional to:

$$F(f) \otimes \sum_{n=-\infty}^{\infty} \delta(f - nF_s) \quad (2.17)$$

This result is easiest interpreted by the graphical representation of convolution (Chapter 13 and Appendix 13.1) which is sliding the Dirac comb ([Fig. 2.6F](#)) along the Fourier transform $F(f)$ ([Fig. 2.6E](#)). At any point in this sliding procedure the impulses in the train sift the value in the Fourier transform $F(f)$. When $F(f)$ lies within the gaps between the individual δ functions, we obtain a periodic function as shown in [Fig. 2.6D](#). This result illustrates the same relationship between sample frequency and highest frequency component in a signal as discussed before. In order for $F(f)$ to fall within the gaps of the δ function train, the highest frequency in signal $f(t)$ must be $< F_s/2$, the Nyquist frequency. If, on the contrary, $F(f)$ does not fall within the gaps of the δ function train there will be an overlap resulting in distortion due to an aliasing effect ([Fig. 2.7](#)).

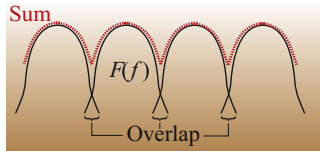


FIGURE 2.7 Equivalent of Fig. 2.6D in the case where the spectra $F(f)$ do not fit within the impulses in the impulse train. This will cause the sum of the individual contributions (red) to include overlap, resulting in an aliasing effect.

2.4 THE MOVE TO THE DIGITAL DOMAIN

Last, but not least, it must be noted that due to the digital revolution most of the functions performed by the analog components of the measurement chain (Fig. 2.1) become redundant or can be moved into the digital domain. With the development of high-resolution ADC, the range of the conversion process becomes large enough that little or no amplification is required in many cases. For example, a 32-bit ADC has a resolution of $2^{32} = 4.295 \times 10^9$ levels. If this is coupled to a 5V range, one can resolve amplitude differences at a 0.23-nV precision without any additional amplification. In addition, high-speed ADC and low-cost storage media allow one to sample so fast that the S/H function is no longer a requirement. The low cost of ADC circuits also allows you to use one converter per data channel, thus eliminating the need for an MUX. Furthermore, faster processors (central processing units, CPUs) and dedicated digital signal processing hardware allow implementation of real-time digital filters that can replace their analog equivalents.

From the above, one might almost conclude that by now we can simply connect an ADC to a biological process and start recording. This conclusion would be wrong since there are two fundamental issues that must be addressed in the analog domain. First, even if the nature of the process is electrical (not requiring a special transducer), there is the impedance conversion issue discussed previously (see Eqs. 2.1 and 2.2). Second, one must deal with the aliasing problem before the input to the ADC. Because most biological processes have a “natural” high-frequency limit, one could argue for omission of the antialiasing step at very high sample rates. Unfortunately, this would make one “blind” to high-frequency artifacts of nonbiological origin, and without subsequent down-sampling it would require huge amounts of storage.

APPENDIX 2.1

In this appendix we address the Fourier transform of a sampled function and investigate the relationship between this transform and the Fourier transform of the underlying continuous time function (see also [Section 2.3](#)). The following discussion is attached to this chapter because the topic of sampling logically belongs here. However, a reader who is not yet familiar with Fourier transform and convolution is advised to read this material after studying Chapters 5–8, 13.

We obtain the sampled discrete time function by multiplying the continuous time function with a train of impulses ([Eq. 2.5](#)). The Fourier transform of this product is the convolution of the Fourier transform of each factor in the product (Chapter 13), i.e., the continuous time function and the train of impulses. This approach is summarized in [Fig. 2.6](#). In this appendix we will first determine the Fourier transform of the two individual factors; then we will determine the outcome of the convolution.

The transform of the continuous function $f(t)$ will be represented by $F(f)$. The Fourier transform $\Delta(f)$ of an infinite train of unit impulses (Dirac comb) is:

$$\Delta(f) = \int_{-\infty}^{\infty} \underbrace{\sum_{n=-\infty}^{\infty} \delta(t - nT_s)}_{\text{train of unit impulses}} e^{-j2\pi ft} dt \quad (\text{A2.1-1})$$

As shown in [Section 2.3](#), we can evaluate this integral by exchanging the order of summation and integration, and by using the sifting property of the δ function for the value nT_s (see [Eq. 2.8](#)):

$$\Delta(f) = \sum_{n=-\infty}^{\infty} e^{-j2\pi fnT_s} = \sum_{n=-\infty}^{\infty} e^{j2\pi fnT_s} \quad (\text{A2.1-2})$$

[Eq. \(A2.1-2\)](#) shows that the exponent's sign can be changed because the summation goes from $-\infty$ to ∞ . First we will consider the summation in [Eq. \(A2.1-2\)](#) as the limit of a summation for $\sum_{n=-N}^N$ with $N \rightarrow \infty$. Second, we use the Taylor series $\left(\frac{1}{1-x} = 1 + x + x^2 + x^3 + \dots\right)$ of the exponential, i.e.:

$$\frac{1}{1 - e^{j2\pi fT_s}} = 1 + e^{j2\pi fT_s} + e^{2j2\pi fT_s} + e^{3j2\pi fT_s} + \dots$$

to create and subtract the following two expressions:

$$\begin{aligned}
 \frac{e^{-j2\pi fNT_s}}{1 - e^{j2\pi fT_s}} &= e^{-j2\pi fNT_s} + e^{-j2\pi f(N-1)T_s} + e^{-j2\pi f(N-2)T_s} + \dots \\
 &= \sum_{n=-N}^{\infty} e^{j2\pi fnT_s} \quad \text{for } -N \rightarrow \infty \text{ range} \\
 \frac{e^{j2\pi f(N+1)T_s}}{1 - e^{j2\pi fT_s}} &= e^{j2\pi f(N+1)T_s} + e^{j2\pi f(N+2)T_s} + e^{j2\pi f(N+3)T_s} + \dots \\
 &= \sum_{n=N+1}^{\infty} e^{j2\pi fnT_s} \quad \text{for } N+1 \rightarrow \infty \text{ range} \\
 \hline
 \frac{e^{-j2\pi fNT_s} - e^{j2\pi f(N+1)T_s}}{1 - e^{j2\pi fT_s}} &= \sum_{n=-N}^N e^{j2\pi fnT_s} \quad \text{for } -N \rightarrow N \text{ range}
 \end{aligned}
 \tag{A2.1-2}$$

Eq. (A2.1-3) is an expression similar to Eq. (A2.1-2), except for the range of summation from $-N$ to N instead of $-\infty \rightarrow \infty$. Subsequently, we multiply both the numerator and denominator in Eq. (A2.1-3) by $e^{-j2\pi fT_s/2}$ and use the Euler relationships $e^{jx} = \cos x + j \sin x$ and $e^{-jx} = \cos x - j \sin x$ to rewrite Eq. (A2.1-3) as follows:

$$\begin{aligned}
 &= \frac{e^{-j2\pi f(N+1/2)T_s} - e^{j2\pi f(N+1/2)T_s}}{e^{-j2\pi fT_s/2} - e^{j2\pi fT_s/2}} = \frac{\sin[(N+1/2)2\pi fT_s]}{\sin[2\pi fT_s/2]} \\
 &= \frac{\sin[(N+1/2)2\pi fT_s]}{\pi f} \frac{\pi f}{\sin[2\pi fT_s/2]}
 \end{aligned}$$

First we will show that the above expression is a periodic function with period $F_s = 1/T_s$. We substitute $f = f + F_s$ for $f + 1/T_s$ in $\frac{\sin[(N+1/2)2\pi fT_s]}{\sin[2\pi fT_s/2]}$ and obtain:

$$\frac{\sin[(N+1/2)2\pi(f+1/T_s)T_s]}{\sin[2\pi(f+1/T_s)T_s/2]} = \frac{\sin[(N+1/2)2\pi fT_s + (N+1/2)2\pi]}{\sin[2\pi fT_s/2 + \pi]}$$

Because a sine function is periodic over 2π , and N is an integer, we observe that both numerator and denominator are sine functions augmented by π ; using $\sin(x + \pi) = -\sin(x)$, we then obtain:

$$= \frac{-\sin[(N+1/2)2\pi fT_s]}{-\sin[2\pi fT_s/2]} = \frac{\sin[(N+1/2)2\pi fT_s]}{\sin[2\pi fT_s/2]}$$

this is the same result as the expression we started with. Therefore, the expression is periodic for $1/T_s$.

Second, the expression must be taken to the limit for $N \rightarrow \infty$ in order to obtain the equivalent of Eq. (A2.1-2). First, we split the equation above into two factors. For $N \rightarrow \infty$ the first factor can be written as $\delta(f)$, i.e.:

$$\lim_{N \rightarrow \infty} \frac{\sin[(N + 1/2)2\pi f T_s]}{\pi f} \frac{\pi f}{\sin[2\pi f T_s/2]} = \delta(f) \frac{\pi f}{\sin[2\pi f T_s/2]} \quad (\text{A2.1-4})$$

We already know that the expression in Eq. (A2.1-4) is periodic over an interval $F_s = 1/T_s$, therefore we can evaluate the behavior of Eq. (A2.1-4) between $-F_s/2$ and $F_s/2$. The δ function is 0 for all $f \neq 0$, therefore we must evaluate the second term in Eq. (A2.1-4) for $f \rightarrow 0$. Using l'Hôpital's rule (differentiate the numerator and denominator, and set f to zero) we find that the nonzero value between $-F_s/2$ and $F_s/2$, for $f = 0$ is:

$$\frac{\pi}{(2\pi T_s/2)\cos[2\pi f T_s/2]} = \frac{1}{T_s}$$

Combining this with Eq. (A2.1-4), we obtain:

$$\frac{1}{T_s} \delta(f) \quad (\text{A2.1-5})$$

This outcome determines the behavior in the period around 0, because the expression in Eq. (A2.1-5) is periodic with a period of $F_s = 1/T_s$, we may include this in the argument of the δ function and extend the result above to read:

$$\frac{1}{T_s} \sum_{n=-\infty}^{\infty} \delta(f - nF_s) \quad (\text{A2.1-6})$$

Combining Eqs. (A2.1-1) and (A2.1-6) we may state that:

$$\sum_{n=-\infty}^{\infty} \delta(t - nT_s) \Leftrightarrow \frac{1}{T_s} \sum_{n=-\infty}^{\infty} \delta(f - nF_s) \quad (\text{A2.1-7})$$

The expressions to the right and left of the \Leftrightarrow in Eq. (A2.1-7) are the time and frequency domain representations of the train of impulses shown in Fig. 2.6B and F.

Finally we return to the original problem of the sampled version of continuous wave $f(t)$ and its Fourier transform $F(f)$. The Fourier transform of the sampled function is the convolution of the Fourier transforms of $f(t)$ with the transform of the train of impulses, i.e.:

$$F(f) \otimes \frac{1}{T_s} \sum_{n=-\infty}^{\infty} \delta(f - nF_s) = \frac{1}{T_s} \int_{-\infty}^{\infty} F(y) \sum_{n=-\infty}^{\infty} \delta(f - nF_s - y) dy$$

The expression after the equal sign is the convolution integral (Chapter 13). Assuming we can interchange the summation and integration:

$$\frac{1}{T_s} \sum_{n=-\infty}^{\infty} \int_{-\infty}^{\infty} F(y) \delta(f - nF_s - y) dy$$

The δ function is even (Appendix 5.1) and may be written as $\delta[y - (f - nF_s)]$. Using the sifting property of the δ function (Eq. 2.8) the integral above evaluates to $F(f - nF_s)$. Finally, we can relate the Fourier transforms of a continuous wave and its sampled version as follows:

$$f(t) \Leftrightarrow F(f) \quad \text{and}$$

$$f(t) \text{ sampled at rate } F_s = 1/T_s \Leftrightarrow \frac{1}{T_s} \sum_{n=-\infty}^{\infty} F(f - nF_s) \quad (\text{A2.1-8})$$

The relationship in Eq. (A2.1-8) is depicted in Fig. 2.6. Compare the continuous transform pair Fig. 2.6A and E with the sampled equivalent in Fig. 2.6C and D.

EXERCISES

2.1 Explain the role of a preamplifier.

2.2 What is the sifting property of the delta function?

2.3 Evaluate the following integrals

a. $\int_{-\infty}^{\infty} e^t \delta(t) dt$

b. $\int_{-\infty}^{\infty} \sin(2\pi\omega t) \delta(t) dt$

c. $\int_{-\infty}^{\infty} \cos(2\pi\omega t) \delta(t) dt$

d. $\int_{-\infty}^{\infty} at \delta(t) dt$

e. $\int_{-\infty}^{\infty} (at^4 - t^3) \delta(t) dt$

2.4 Evaluate the same integrals in 2.3 after replacing $\delta(t)$ with $\delta(t-2)$.

2.5 What is aliasing?

References

- Ingle, V.K., Proakis, J.G., 1997. Digital Signal Processing Using MATLAB V.4. PWS Publishing Company, Boston.
- Wallisch, P., Lusignan, M.E., Benayoun, M.D., Baker, T.I., Dickey, A.S., Hatsopoulos, N.G., 2014. MATLAB for Neuroscientists: An Introduction to Scientific Computing in MATLAB, second ed. Academic Press, Amsterdam.
- An excellent introduction to the use of MATLAB with many simple as well as advanced examples.*